Finite element modelling of 3D printed bioresorbable polymer stent deployment

Irina V. Khaydukova, Gang Shen, Eoin O'Cearbhaill

UCD Centre for Biomedical Engineering, School of Mechanical and Materials Engineering, University College Dublin, Ireland

2023 UCD STEM SYMPOSIUM, June 13, 2023

Abstract

Current options for paediatric stenting of aortic coarctation do not provide patient-specific design, growth accommodation and may require reintervention. The use of bioresorbable polymer stents would allow the implant to degrade by the time the artery grows significantly. The choice of design for high radial strength and low recoil requires stent finite element (FE) modelling. The implementation of 3D printing could give the possibility for bespoke stent designs but their performance must also be preliminary evaluated in-silico.

The current objective was the development of a FE model of polymer stent deployment procedure. The experimental evaluation of stent recoil was performed on a 3D printed stent from poly-lactic acid (PLA). The FE modelling compared two main approaches to polymer stent modelling in Abaqus: stent expansion based on displacement of a symmetric part of geometry and a dynamic whole stent deployment on a tri-fold balloon. The evaluated parameters included plastic strain localisation, recoil, dogboning and foreshortening of the stent.

The two models differed significantly in plastic strain distribution. In pressure model it was concentrated in zig-zag connections which is closer to the experimental crack locations during stent overexpansion or high-speed deployment. Dynamic model is also more suitable because it captures the dogboning effect. The FE recoil was similar in both models, and it was 0.2 mm less than the experimental value. Further improvements of the model including experimental evaluation of PLA material and additional deployment tests could increase the accuracy. Future directions also include PLA/Poly(ε-caprolactone) 3D printing and other stent geometries.

Materials

PLA material parameters for the FEA were approximated from the true stress-strain value from (Wang Qian et al., 2017) (Table 1 and Figure 1) and noncloMpliable balloon parameters from (Mazurkiewicz Ł.A., 2021).

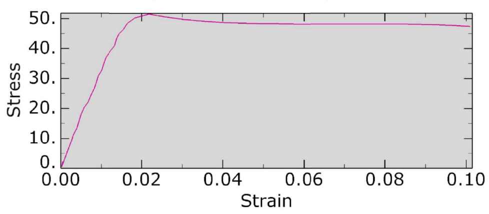

Figure 1. Approximated PLA properties for FEA

Table 1. Material parameters for FEA

Parameter	Value
Stent – PLA (Elastic-plastic model)	
Young's modulus, MPa	3142.04
Ultimate tensile strength, MPa	47.4291
Density, g/mm³	0.00124
Poisson's ratio	0.3
Balloon (linear elastic model)	
Young's modulus, MPa	900
Density, g/mm³	0.0011
Poisson's ratio	0.3

Methods

3D printing

A zig-zag shaped stent was manufactured using a proposed method of Fused Filament Fabrication on rotation mandrel based on direct extrusion path generation from parametric curves generated with Grasshopper (Gurminder Singh, 2022)(Figure 2) with the parameters in Table 2.

Table 2. 3D printing parameters

Parameter	Value
Extrusion temperature, °C	220
Nozzle speed, mm/min	300
Extrusion value	0.009
Stent length, mm	21.7
Strut width, mm	0.33
Strut thickness, mm	0.2

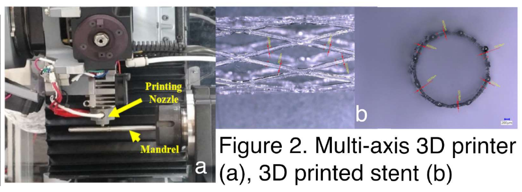

Figure 2. Multi-axis 3D printer (a), 3D printed stent (b)

Finite element modelling

Displacement deployment (Abaqus Standard)

The first model reviewed the displacement-based approach for deployment. A 1/12th part of stent was modelled as a deformable shell with thickness of 0.2 mm in Standard analysis with symmetry constraints in circumferential and longitudinal directions (Figure 3a).

1 step: Displacement constraint applied to the stent inner surface with 2.6 mm displacement outwards for 0.3 s.

2 step: Removal of displacement constraint for 0.3 s.

Pressure deployment (Abaqus Explicit)

In pressure controlled approach the stent was modelled was a deformable solid with thickness of 0.2 mm in Abaqus Explicit. The balloon was modelled as a tri-fold deformable shell with thickness of 0.02 mm (Figure 3b,c).

1 step: Gradually increasing pressure to 0.2 MPa applied to the inner surface of balloon for 0.3 s.

2 step: Pressure instantly set to 0 MPa and then gradually decreased to -0.03 MPa for 0.3 s.

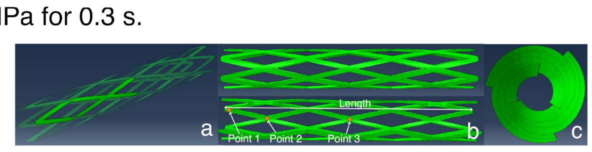

Figure 3. CAD model for FEA: 1/12 part of stent (Abaqus Standard). The transparent part of the stent is presented for visualization purposes and was not modelled (a). Stent geometry in pressure analysis (Abaqus Explicit). Lower image is the same stent with a longitudinal cut showing points and length used for analysis (b). Trifolded balloon (Abaqus Explicit) (c)

Results

Experimental test

A 3D printed stent was mounted on the balloon "CRE Fixed Wire" and the pressure in the balloon was slowly increased to 0.2 MPa and then rapidly decreased (Figure 4). The maximum internal diameter of the stent was recorded as the external diameter of the balloon (8 mm). Stent recoil was equal to 0.7 mm (8.7 %).

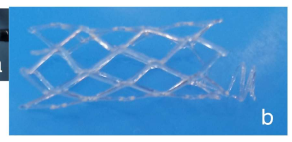

Figure 4. Stent at the maximum deployed state on the balloon (a) and after expansion (b)

FEA results

Displacement deployment (Abaqus Standard)

In displacement analysis the stent dogboning was not applicable as the whole stent displaced simultaneously. Stent maximum diameter was 8,2 mm, stent recoil was equal to 0.42 mm (5.2 %). The distribution of equivalent plastic strain is indicated in Figure 5.

Figure 5. Stent at its maximum expansion: whole geometry (a), 1/12 part of geometry (b)

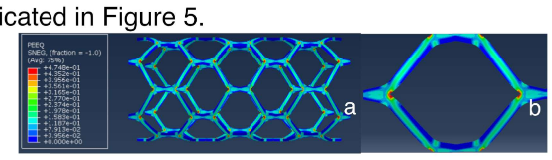

Pressure deployment (Abaqus Explicit)

Stent maximum diameter was 8.02-8.19 mm, stent recoil was equal to 0.42-0.44 mm (5.2-5.4 %) (Figure 6). Lower values correspond to the center - Point 3, higher - to the end - Point 2.

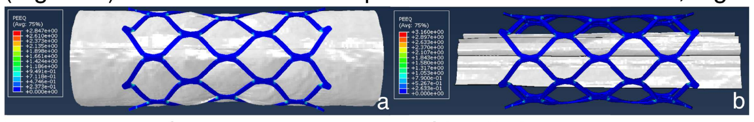

Figure 6. Stent maximum diameter (a) and recoil (b)

The plastic deformation was localised in all zig-zag connection. However, the plastic strain at the ends appeared first and had the largest value. The equivalent plastic strain is shown in Figure 7 (blue regions indicate the absence of plastic deformation).

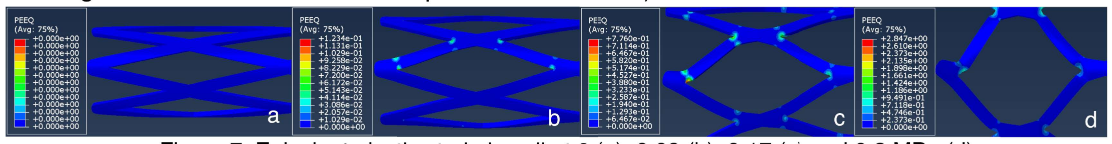

Figure 7. Eqivalent plastic strain in cell at 0 (a), 0.09 (b), 0.17 (c) and 0.2 MPa (d)

The pressure analysis with tri-fold balloon allows for the estimation of dogboning (the effect of unequal stent diameter at the center and at the end during deployment and recoil) (Figure 8a-c). The dogboning was estimated at Point 1 and Point 3. For stent foreshortening, the whole length of the stent was evaluated (Figure 8d). The dogboning, foreshortening and recoil were calculated according to (Abbaslou, M., 2023).

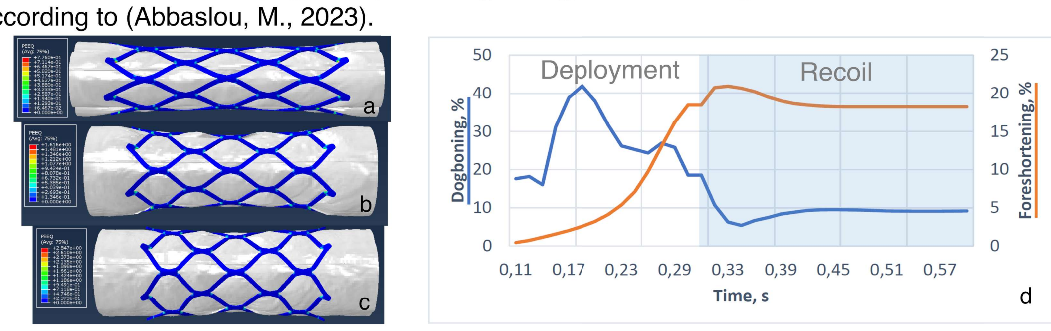

Figure 8. Stent expansion process at 0.15 (a), 0.18 (b) and 0.2 MPa (c). Dogboning and foreshortening (d)

Due to the dogboning effect, the stent is at first expanded at the ends for 0.3 s. Then at 0.3 s the diameter at Point 1 is maximum (8.44 mm). However, when the pressure drops, the stent stabilises its diameter and therefore the diameter in the center continues to increase while the diamter at the ends decrease. Thus the stent attains its maximum diameter at the center at 0.33-0.34 s.

Conclusion

Both displacement and pressure FE models give similar results in terms of recoil value. However, the **experimental recoil was larger** (8.7 compared to 5.2 %) which may have following reasons:

1) In litterature PLA parameters vary significantly (Young's modulus can be in the range of 2.2-3.5 MPa). Therefore, further experimental **evaluation of PLA material** is needed.

2) The experimental tests should be repeated with a **tri-fold balloon catheter** for stent deployment with which is not compliant and gives more uniform expansion. The current catheter could give larger experimental recoil.

3) The result of only one stent sample was used for the stent deployment and recoil test. Other **tests are requied** to establish the mean value of recoil.

Two models vary significantly in **plastic strain distribution**. In pressure model it was concentrated in zig-zag connections and displacement model showed more uniform distribution, which can be related to uniform expansion. High stress and strain concentrations at connection points appear closer to reality because the **cracks in stent structure during stent overexpansion** or high-speed deployment are also situated in these areas.

The displacement-based deployment does not allow to evaluate the **dogboning effect**, which is an important parameter for polymer stents. The Dynamic analysis is also more suitable, as in converges easier for **large deformations and nonlinear materials**.

Future directions

1. Tensile tests of PLA:
   - Strut samples
   - Dumbbel-shaped samples
2. Additional tests with registration of foreshortening and recoil
3. 3D printing of stents from PLA/Poly(ε-caprolactone)(PLC) blend (Figure 9)
4. Tests (3D printing and FEA) of other stent designs

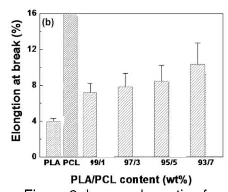

Figure 9. Larger elongation for PLA/PCL blends

Acknowledgement

This study was supported by the National Children's Research Center (Paediatric Research Project Grants number PRPG/H/18/320)